AIAA JOURNAL
Vol. 46, No. 1, January 2008

Technical Notes

TECHNICAL NOTES are short manuscripts describing new developments or important results of a preliminary nature. These Notes should not exceed 2500 words (where a figure or table counts as 200 words). Following informal review by the Editors, they may be published within a few months of the date of receipt. Style requirements are the same as for regular contributions (see inside back cover).

Modified Expression for Critical Reynolds Number in Eccentric Taylor–Couette Flow

T. T. Lim* and S. S. Lim†
National University of Singapore, Singapore 119260, Republic of Singapore

DOI: 10.2514/1.29323

Nomenclature

d	=	mean gap width between two cylinders
e	=	displacement of the centers of the outer and inner cylinders
H	=	height of fluid column
Re	=	$R_i\Omega d/\nu$
Re_c	=	critical Reynolds number
Re_{co}	=	critical Reynolds number at zero eccentricity
R_i	=	outer radius of the inner cylinder
R_o	=	inner radius of the outer cylinder
Ta_c	=	critical Taylor number
Γ	=	aspect ratio (H/d)
δ	=	clearance ratio $(Ro - Ri)/Ri$
ε	=	eccentricity (e/d)
η	=	mean radius ratio (R_i/R_o)
λ_c	=	critical axial wavelength
ν	=	kinematic viscosity
Ω	=	angular velocity, rad/s

I. Introduction

TAYLOR–COUETTE flow (TCF) has been a cornerstone of concepts of hydrodynamic stability and origins of turbulence in fluid physics and also of great importance in various fields of engineering. Since Taylor's pioneering work in 1923 [1], numerous related studies have been conducted and extensive reviews of this flow problem can be found in [2–6]. In the mid-1900s, the stability of a viscous flow within the annulus of a rotating inner cylinder and a stationary, eccentrically arranged outer cylinder was first considered experimentally and theoretically. By displacing the axes of the inner and outer cylinders away from each other while maintaining the same basic geometry, the rotation of the inner cylinder gives rise to a varying, circumferential pressure gradient. This results in a combined Couette and pressure flow around the inner cylinder that modifies the conventional TCF problem significantly.

Received 15 December 2006; revision received 14 August 2007; accepted for publication 5 September 2007.

*Professor, Department of Mechanical Engineering, 10 Kent Ridge Crescent.

†Graduate Student, Department of Mechanical Engineering, 10 Kent Ridge Crescent.

Akin to the concentric case, eccentric TCF also undergoes transition from circular Couette flow (CCF) to Taylor vortex flow (TVF) as instability sets in with increasing Reynolds number (Re). TVF is brought about by the action of centrifugal forces which cause the development of a secondary circulatory flow pattern in the form of toroidal vortices spaced periodically in the axial direction. The development of these vortices leads to increased frictional losses and load capacity and hence, it is of significant importance to identify the transition point at various eccentricities.

Cole [7,8] pioneered the study of eccentric TCF by determining the critical Taylor number (Ta_c) at the onset of instability using torque measurement for eight radius ratios between 0.630 and 0.954 at various eccentricities. In his study, Ta_c was found to increase substantially with eccentricity and he concluded that eccentricity was a stabilizing factor in TCF. His finding was supported by subsequent experimental studies [9,10] as well as theoretical studies [11–14].

In another paper, Castle and Mobbs [15] described the presence of two stages of instability during transition to TVF for eccentric cylinders. The onset of the "first instability" was found to occur at Ta_c smaller than that of the concentric case up to eccentricity of 0.4. Thereafter, Ta_c rose substantially above the initial value. A similar trend was also described in [16,17]. On the other hand, Ta_c corresponding to the onset of the "second instability" indicated a stabilizing effect of eccentricity similar to the conclusion made by Cole [7,8] and more recently by Xiao et al. [18].

In their theoretical analysis of eccentric Taylor–Couette flows, Eagle et al. [13] derived a mathematical expression $Ta_c = 1694.97(1 + 1.1618\delta)(1 + 2.6185\varepsilon^2)$ which relates the onset of Taylor vortices or critical Taylor number (Ta_c) to the eccentricity (ε) and clearance ratio (δ) between the inner and outer cylinders. The equation is based on the assumption of small eccentricity and clearance ratio, and compares favorably with the experiments [9,15,19] up to $\varepsilon \approx 0.4$, but deviates significantly at high eccentricity. In terms of Reynolds number, the above equation can also be expressed as

$$\frac{Re_c}{Re_{co}} = \sqrt{1 + 2.6185\varepsilon^2}$$

The present study is motivated by the lack of agreement between the theory and experiment at high eccentricity, and the aim here is to determine experimentally an alternative expression that will give a more realistic representation of the effect of eccentricity on the onset of Taylor vortices. As far as we are aware, this equation currently does not exist and will provide a useful means of evaluating the critical Reynolds numbers more effectively for a much wider range of eccentricity.

II. Experimental Setup

The present experiments were performed using a rheometer (an instrument which is commonly used to measure rheological properties of fluids) and a modified version of the apparatus used by Lim and Tan [20] to study torque characteristics of the Taylor–Couette flow between two concentric cylinders. A schematic drawing of the experimental apparatus using a HAAKE RS75 rheometer is shown in Fig. 1 and only the essential features will be described here. The base support has a base diameter of 48 mm that matches the diameter of the mounting hole of the measurement table of the rheometer. The diameter at the top of the

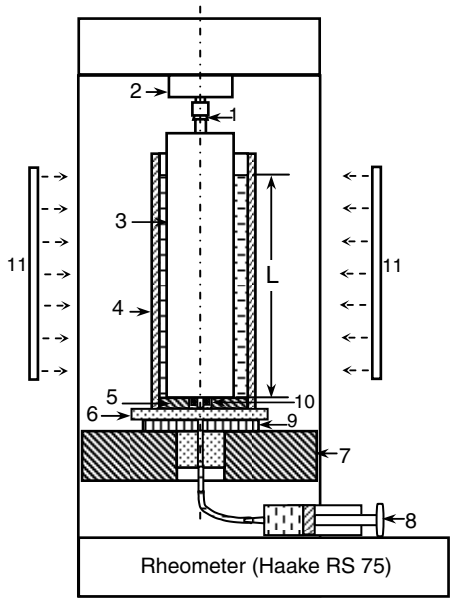

Fig. 1 A schematic drawing of the experimental apparatus using a Haake RS 75 Rheometer. 1: Cone; 2: air bearing and load cell; 3: inner cylinder; 4: outer cylinder; 5: base disk; 6: base support: 7: movable support; 8: syringe; 9: fastener; 10: precision bearing; 11: flourescent lightingsl L = liquid level.

base support is increased to 65 mm so that the apparatus, when assembled, is fixed firmly on the top of the measurement table. It has a circular protrusion with a diameter of 13 mm and a height of 4 mm located centrally on the top surface. A precision ball bearing is inserted into the circular protrusion to provide support for the inner cylinder and at the same time allows the inner cylinder to rotate with minimal friction. The base support also has a small opening at the bottom where the working solution is introduced into the annulus by means of a syringe when the parts are fully assembled. This technique prevents any air bubbles from getting trapped underneath the inner cylinder which may lead to erroneous results and also allows an accurate control of the height of the fluid column.

The base disk has a hole with a diameter of 13 mm which allows it to slide fit onto the circular protrusion located on the top of the base support. When attached together, the upper surfaces of the disk and the circular protrusion are flushed. The purpose of the base disk is to alter the alignment of the axes of the inner and the outer cylinder to obtain the required eccentricity in the experiment. This is achieved by varying the distance between the center of the hole and the center of the disk.

Three outer cylinders, all fabricated from Plexiglas, were used in this experiment. They have inner radii (R_o) of 16.79 ± 0.05 mm, 18.84 ± 0.05 mm, and 20.98 ± 0.05 mm, respectively, and a common height of 110 mm. The aluminum inner cylinder has a radius of (R_i) 15.11 ± 0.05 mm and height of 95 mm. It is coated with a thin layer of black paint to achieve better flow visualization during image recording. The top of the cylinder is reduced to a shaft with a diameter of 10 mm that has a cone-shaped fitting at its end to allow the cylinder to be attached rigidly to the drive shaft of the rheometer. It has a small, conical stud at the bottom that can be inserted into the precision ball bearing on the base support when assembled. The purpose of the stud is to ensure that the alignment of the vertical axes of the inner and the outer cylinders is maintained consistently. Together with the precision ball bearing, it ensures that the inner cylinder rotates with minimal friction and lateral oscillation.

The rotational motion of the inner cylinder is driven by an extremely low inertia torque motor located within the rheometer. The cylinder is connected to the drive shaft of the motor which is centered by an air bearing, which ensures a virtually frictionless transmission of the rotational motion to the inner cylinder. The torque on the inner cylinder is measured based on the current going into the motor. By establishing the dependence of the applied current and the resultant torque, accurate measurement of the torque is achieved. The angular velocity is measured optically using a line disk connected to the drive shaft. The disk generates 1×10^6 impulses per revolution. These impulses are detected and processed by a digital encoder which enables the rheometer to measure angular velocity at a high degree of accuracy. The maximum attainable angular velocity of the rheometer is 57.6 rad/s.

The flow within the annulus is characterized by the following parameters: 1) the mean radius ratio $\eta = R_i/R_o$, 2) the eccentricity $\varepsilon = e/d$, 3) the Reynolds number $Re = R_i\Omega d/\nu$, and 4) the aspect ratio $\Gamma = H/d$. In the present study, the radius ratios (η) of 0.72, 0.80, and 0.90 were considered with the aspect ratios (Γ) of 15 and 25, and eccentricities (ε) from 0.0 to 0.8, thus giving a total of 36 sets of results. The choice of the aspect ratio was dictated by the height of the cylinders, which is constrained by the physical size of the rheometer. The working solution was a homogeneous mixture of glycerin, distilled water, and Kalliroscope solution. 40% of glycerin and 60% of distilled water in weight were first mixed together, before 10% of a Kalliroscope AQ-1000 reflective flakes solution in volume was added to the mixture for flow visualization purposes. Lim and Tan [20] were able to achieve good quality flow images using a similar mixture in their flow visualization studies. Tests conducted by them using concentration up to 15% in volume of a Kalliroscope solution showed that the working solution was still Newtonian. The dynamic viscosity (μ) of the working solution was determined to be 3.4×10^{-3} kg/ms using the same HAAKE RS75 rheometer and the double gap cylinder sensor DG41 recommended by the manufacturer, and the density (ρ) of the working solution was measured to be 1086 kg/m^3 using a density bottle of a known volume. Thus, the kinematic viscosity (ν) of the working solution was calculated to be about 3.13×10^{-6} m^2/s, which is about 3.13 times higher than that of water.

Torque measurement was carried out using a multistep procedure provided in the rheometer program. The angular velocity of the inner cylinder was increased from rest to approximately 57 rad/s in discrete steps. In addition, the rheometer was programmed to collect a total of 100 data points within this range for each measurement. Hence, the step increment in angular velocity was approximately 0.57 rad/s. At each data point, the angular velocity of the inner cylinder, the torque exerted on the inner cylinder, and the time elapsed after the commencement of the experiment, were recorded by the rheometer. In addition, all experiments were conducted in an air-conditioned room with a temperature of approximately 22°C. A heat circulator was attached to the rheometer to maintain the temperature of the working fluid at a constant value during the experiments.

As the angular velocity of the inner cylinder was increased, the flow within the annulus transited through different states. Concurrent with the torque measurement, the resulting flow patterns, made visible by the Kalliroscopic reflective flakes in the working solution, were captured using a charge-coupled device (CCD) color video camera and a video cassette recorder (VCR) equipped with a time-code card and used for subsequently analysis. Simultaneously, the time elapsed after the start of the experiment was also encrypted within the super video home system (SVHS) videotapes during recording using the time-code card installed in the VCR. As mentioned previously, an identical parameter was also recorded by the rheometer and they were used jointly to relate the changes in torque measurements to the changes in flow states.

In the present study, a torque measurement technique [7–10,15] was initially adopted to determine the critical Reynolds number. With this technique, the onset of Taylor vortices is explicitly marked by a sudden increase in the gradient (or "kink") of the torque-speed curve. The rotational speed at the kink can then be used to evaluate the critical Reynolds number. In the course of the experiment, it was discovered that the kink was not so evident at high eccentricity. The transition was more gradual which increased the uncertainties in evaluating the critical Reynolds number. This could explain why some of the published data in the literature show considerable scatter at high eccentricities when the torque measurement technique was used [8–10,15]. In view of this, the flow visualization technique was

subsequently adopted to identify the critical Reynolds number for all cases. Here, the flow is deemed critical when the Taylor vortices filled the entire fluid column as the inner cylinder rotates (see Fig. 2). The rotational speed of the inner cylinder at this particular instant was recorded and used to determine the corresponding critical Reynolds number. This method has been successfully employed in [10,15,16,19]. Furthermore, our results obtained at low eccentricities also agree very well with that obtained using torque measurements, thus verifying the accuracy of the flow visualization technique. For example, the critical Reynolds numbers (Re_c) for the onset of the Taylor vortices for $\eta = 0.80$, $\varepsilon = 0.0$ obtained using flow visualization and torque measurement were 93.4 and 95, respectively. Likewise, for the same radius ratio, the critical Reynolds numbers for $\varepsilon = 0.1$ were, respectively, 103.8 and 104.

III. Results and Discussion

To ascertain the accuracy of the apparatus, experiments were first conducted for the concentric cylinders ($\varepsilon = 0$) with $\eta = 0.72$, 0.80, and 0.90, and the critical Reynolds numbers (Re_c) for these cases were 81.8, 93.4, and 121.5, respectively. These results are in good agreement with the published data [21–23], thus verifying the accuracy of the present experiment.

For the case of eccentric cylinders, measurements were conducted for eccentricities ranging from 0.1 to 0.8 for each of the three radius ratios. Each flow condition was repeated 3 times to ensure reproducibility of the results. The critical Reynolds number (Re_c) was accurate to 3% at zero eccentricity, but deteriorated to a maximum of 6% at the largest eccentricity of 0.8. The results when plotted in nondimensional form with $(Re_c/Re_{co})^2 - 1$ versus eccentricities (ε) is presented in Fig. 3. Previous published experimental data [7–9,19] are also included for comparison. It can be seen from the figure that, within the experimental accuracy, our results exhibit good agreement with the earlier works. Although the experimental data generally collapse onto a single curve up to $\varepsilon \approx 0.4$, there is a noticeable scatter at higher eccentricity, probably caused by the increased uncertainty in determining Re_c from different sources. Nevertheless, the "collapse" in the data confirms the theoretical prediction that Re_c/Re_{co} is independent of the radius ratio, clearance ratio, and aspect ratio. The trend line shown in the figure represents the theoretical expression

$$\frac{Re_c}{Re_{co}} = \sqrt{1 + 2.6185\varepsilon^2}$$

obtained by Eagle et al. [13]. Although the theory agrees very well with the experiment up to $\varepsilon \approx 0.4$, it breaks down at higher eccentricity. Using a similar power-law formulation to curve fit the experimental data in Fig. 3 gives the curve of best fit of

$$\left(\frac{Re_c}{Re_{co}}\right)^2 - 1 = 32.1\varepsilon^{5.844}$$

or

$$\frac{Re_c}{Re_{co}} = \sqrt{1 + 32.1\varepsilon^{5.844}}$$

However, if the power index of ε is rounded up to the same degree of accuracy as the theoretical value, it leads to

$$\frac{Re_c}{Re_{co}} = \sqrt{1 + 32.1\varepsilon^6}$$

To the best of our knowledge, this equation has not been reported before and is effective in evaluating Re_c up to $\varepsilon \approx 0.8$. Although not presented here, the present study agrees with Koschmieder [19] that the wavelength of the Taylor vortices (λ_c) decreases substantially for $\varepsilon > 0.4$.

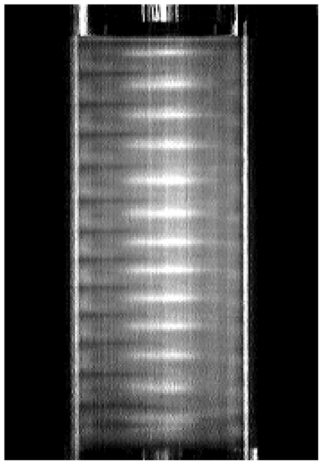

Fig. 2 Taylor vortices at the critical Reynolds number for $\eta = 0.80$, $\Gamma = 25$, $\varepsilon = 0.5$, and $Re_c = 1.33Re_{co}$.

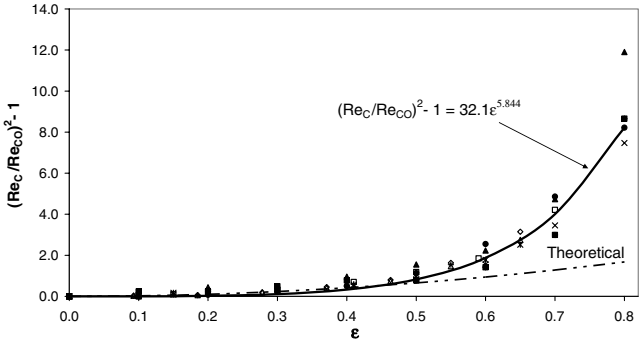

Fig. 3 A plot of $(Re_c/Re_{co})^2 - 1$ versus ε. ▲: Present result ($\eta = 0.72$, $\delta = 0.388$, $\Gamma = 15$); ◆: present result ($\eta = 0.80$, $\delta = 0.247$, $\Gamma = 15$); ■: present result ($\eta = 0.80$, $\delta = 0.247$, $\Gamma = 25$); ●: present result ($\eta = 0.90$, $\delta = 0.111$, $\Gamma = 15$); ◇: Koschmieder (1976) ($\eta = 0.727$, $\Gamma = 52$); △: Koschmieder (1976) ($\eta = 0.727$, $\Gamma = 38$); □: Vohr (1968) ($\eta = 0.91$, $\Gamma = 124$); ×: Cole (1967) ($\eta = 0.83$, $\Gamma = 54$); *: Cole (1969) ($\eta = 0.63$, $\Gamma = 14$); +: Cole (1969) ($\eta = 0.95$, $\Gamma = 115$); solid line: empirical and dash-dotted line: theoretical (based on $Re_c/Re_{co} = \sqrt{1 + 2.6185\varepsilon^2}$).

IV. Conclusions

In this Technical Note, we show that

$$\frac{Re_c}{Re_{co}} = \sqrt{1 + 32.1\varepsilon^6}$$

gives a more realistic representation for the onset of Taylor vortices in an eccentric Taylor–Couette flow than the theoretical expression,

$$\frac{Re_c}{Re_{co}} = \sqrt{1 + 2.6185\varepsilon^2}$$

This empirical equation, which has not been reported before, provides a valuable means of evaluating Re_c more effectively up to $\varepsilon \approx 0.8$. Moreover, it gives an important clue that in any theoretical analysis, the dependency of the critical Reynolds number on eccentricity must be taken to order $\mathcal{O}(\varepsilon^6)$ to have a reasonable representation of the real situation.

References

[1] Taylor, G. I., "Stability of a Viscous Fluid Contained Between Rotating Cylinders," *Philosophical Transactions of the Royal Society of London, Series A: Mathematical and Physical Sciences*, Vol. 223, Feb. 1923, pp. 289–343. doi:10.1098/rsta.1923.0008

[2] Chandrasekhar, S., *Hydrodynamic and Hydromagnetic Stability*, Clarendon Press, Oxford, 1961.

[3] DiPrima, R. C., and Swinney, H. L., "Instability and Transition in Flow Between Concentric Rotating Cylinders," *Hydrodynamics Instabilities and the Transition to Turbulence*, edited by H. L. Swinney, and J. P. Gollub, Vol. 45, Springer Proceedings in Topics in Applied Physics, Springer, Berlin, 1992.
[4] Kataoka, K., "Taylor Vortices and Instabilities in Circular Couette Flow," *Encyclopedia of Fluid Mechanics*, edited by N. P. Cheremisinoff, Vol. 1, Gulf Publication, Houston, 1986, pp. 236–274.
[5] Chossat, P., and Iooss, G., *The Couette-Taylor Problem*, Springer–Verlag, New York, 1994.
[6] Koschmieder, E. L., "Benard Cells and Taylor Vortices," Cambridge Univ. Press, New York, 1993.
[7] Cole, J. A., "Taylor Vortices with Eccentric Rotating Cylinders," *Nature (London)*, Vol. 216, Dec. 1967, pp. 1200–1202. doi:10.1038/2161200b0
[8] Cole, J. A., "Taylor Vortices with Eccentric Rotating Cylinders," *Nature (London)*, Vol. 221, Jan. 1969, pp. 253–254. doi:10.1038/221253a0
[9] Vohr, J. H., "An Experimental Study of Taylor Vortices and Turbulence in Flow Between Eccentric Rotating Cylinders," *Transactions of the ASME: Journal of Lubrication Technology*, Vol. 90, Jan. 1968, pp. 285–296.
[10] Castle, P., Mobbs, F. R., and Markho, P. H., "Visual Observations and Torque Measurements in the Taylor Vortex Regime Between Rotating Eccentric Cylinders," *Transactions of the ASME: Journal of Lubrication Technology*, Vol. 93, Jan. 1971, pp. 121–129.
[11] DiPrima, R. C., and Stuart, J. T., "Non-Local Effects in the Stability of Flow Between Eccentric Rotating Cylinders," *Journal of Fluid Mechanics*, Vol. 54, Pt. 3, 1972, pp. 393–415. doi:10.1017/S0022112072000758
[12] DiPrima, R. C., and Stuart, J. T., "The Nonlinear Calculation of Taylor Vortex Flow Between Eccentric Rotating Cylinders," *Journal of Fluid Mechanics*, Vol. 67, Pt. 1, 1975, pp. 85–111. doi:10.1017/S0022112075000183
[13] Eagle, P. M., Stuart, J. T., and DiPrima, R. C., "The Effects of Eccentricity on Torque and Load in Taylor Vortex Flow," *Journal of Fluid Mechanics*, Vol. 87, Pt. 2, 1978, pp. 209–231. doi:10.1017/S002211207800155X
[14] Masayuki, O., "Stability of Flow Between Eccentric Rotating Cylinders," *Journal of the Physical Society of Japan*, Vol. 58, No. 7, 1989, pp. 2355–2364. doi:10.1143/JPSJ.58.2355
[15] Castle, P., and Mobbs, F. R., "Hydrodynamic Stability of the Flow Between Eccentric Rotating Cylinders: Visual Observations and Torque Measurements," *Proceedings of the Institution of Mechanical Engineers*, Vol. 182, 1968, pp. 41–52.
[16] Versteegen, P. L., and Jankowski, D. F., "Experiments on the Stability of Viscous Flow Between Eccentric Rotating Cylinders," *Physics of Fluids*, Vol. 12, No. 6, 1969, pp. 1138–1143. doi:10.1063/1.1692643
[17] Frenem, J., and Godet, M., "Transition from Laminar to Taylor Vortex Flow in Journal Bearings," *Tribology*, Vol. 4, Nov. 1971, pp. 216–217. doi:10.1016/0041-2678(71)90074-1
[18] Xiao, Q., Lim, T. T., and Chew, Y. T., "Experimental Investigation on the Effect of Eccentricity on Taylor-Couette Flow," *Proceedings of the Tenth International Symposium on Transport Phenomena in Thermal Science and Process Engineering*, edited by K. Suzuki, R. Echigo, and F. Ogino, 1977, Vol. 3, pp. 685–689.
[19] Koschmieder, E. L., "Taylor Vortices Between Eccentric Cylinders," *Physics of Fluids*, Vol. 19, No. 1, 1976, pp. 1–4. doi:10.1063/1.861322
[20] Lim, T. T., and Tan, K. S., "A Note on Power-Law Scaling in a Taylor-Couette Flow," *Physics of Fluids*, Vol. 16, No. 1, 2004, pp. 140–144. doi:10.1063/1.1631417
[21] Coles, D., "Transition in Circular Couette Flow," *Journal of Fluid Mechanics*, Vol. 21, Pt. 3, 1965, pp. 385–425. doi:10.1017/S0022112065000241
[22] Debler, W., Füner, E., and Schaaf, B., "Torque and Flow Patterns in Supercritical Circular Couette Flow," *Proceedings of the 12th International Congress of Applied Mechanics*, edited by M. Hetényi and W. G. Vincenti, Springer, Berlin, 1969, pp. 158–178.
[23] Zarti, A. S., and Mobbs, F. R., "Wavy Taylor Vortex Flow Between Eccentric Rotating Cylinders," *Energy Conservation Through Fluid Film Lubrication Technology: Frontiers in Research and Design*, ASME, New York, 1979, pp. 103–116.

R. Rangel
Associate Editor